On the stability of spectral methods for the homogeneous Boltzmann equation*

Lorenzo PARESCHI[†], Giovanni RUSSO[‡]

Abstract

In this paper we introduce a new smoothed scheme derived from the spectral Fourier method for the homogeneous Boltzmann equation recently introduced in [14, 15]. More precisely we show that using suitable smoothing filters the method can be designed in such a way that the spectral solution remains positive in time and preserves the total mass. Several numerical examples are given to illustrate the previous analysis.

Key words: Boltzmann equation, spectral methods, smoothing tecniques.

1 Introduction

The numerical solution of the Boltzmann equation has been a challenge for several decades. The main difficulties that are encountered concern the high dimensionality of the problem (the density function f depends in general on seven independent variables, namely position, velocity, and time), and the evaluation of the collisional integral. Even when considering space homogeneous problems, it is not easy to construct a scheme that is accurate and maintains most of the qualitative properties of the solution to the equation (such as positivity, conservation of the moments, entropy inequality, and so on).

Monte Carlo schemes can be constructed, which maintain some of the properties (positivity and conservation of the moments) [1]. They are very popular because of their efficiency and flexibility. Unfortunately, because of the statistical fluctuations, they are very inaccurate for non stationary computations.

*This work was partially supported by TMR project "Asymptotic Methods in Kinetic Theory", Contract Number ERB FMRX CT97 0157, and partially by CNR, grant # 97.01030.CT01.

[†]Universitá di Ferrara, Dipartimento di Matematica, Via Machiavelli, 35, 44100 Ferrara, Italy. E-mail: pareschi@dm.unife.it

[‡]Universitá di L'Aquila, Dipartimento di Matematica, Via Vetoio, Loc. Coppito, 67010 L'Aquila, Italy. E-mail: russo@univaq.it

Several deterministic schemes have been constructed, which satisfy many properties of the Boltzmann equation [10, 17]. However, the accuracy of such schemes is quite low, and the computational complexity is large enough, so that for most applications they are not preferred to Monte Carlo-based schemes.

In recent years the simplified Fourier representation of the collisional kernel for Maxwell molecules has gained a lot of popularity (see [2]). Numerically, the idea of using such simplification simply by replacing the continuous Fourier transform by the discrete Fourier transform has been applied by several authors [3, 12, 8].

Only recently [14, 15] it has been developed a general theory on spectral methods for arbitrary collision kernels that can be used to construct effective schemes for the numerical solution of the Boltzmann equation. In particular, in [15] the authors have shown that using such an approach spectral accuracy can be achieved.

The numerical solution obtained by spectral schemes will suffer the loss of some of the properties of the solution, such as positivity and exact conservation of momentum and energy. On the other hand, because of the spectral accuracy of the solution, the error in the moments or the positivity error are spectrally small.

As a general principle, in the numerical solution of the Boltzmann equation, there seems to be a trade-off between accuracy and preservation of properties: if a scheme preserves all the physical properties it is not very accurate. For Monte-Carlo methods this is obvious, whereas for deterministic schemes this is mainly due to the usage of regular grids that poorly approximate the spherical symmetries of the true collision operator.

In this paper we consider the problem of lacking of positivity of the spectral-Fourier method introduced in [14] and studied in [15].

We show that using suitable filtering tecniques, a scheme that preserves positivity of the solution can be constructed. However, the high accuracy property of the scheme can be lost. We perform some numerical test that shows that the loss of positivity of the unsmoothed scheme is spectrally small, and that the cause of negativity (for the unsmoothed scheme) or poor accuracy (for the smoothed scheme) of the solution are essentially due to the negativity or poor accuracy of the initial condition.

2 The spectral Fourier method

As it is usually done for a kinetic equation of Boltzmann type, after a splitting between the convective part and the homogeneous part of the equation, one reduces to study a space homogeneous problem [6]

$$\begin{aligned} &\frac{\partial f}{\partial t} = Q(f,f), \qquad v \in \mathbb{R}^3,\, t>0, \\ &f(v,t=0) = f_0(v). \end{aligned} \tag{1}$$

In (1), $f = f(v,t)$ is a non negative function describing the time evolution of the distribution of particles which move with velocity v at time t.

The first step in the derivation of the Fourier spectral method, as presented in [14, 15], is given by the possibility to represent the collision operator $Q(f,f)$ in (1) as

$$Q(f,f)(v) = \int_{\mathbb{R}^3}\int_{S^2} \beta(|q|,\theta)[f(v+q^+)f(v+q^-) - f(v)f(v+q)]\,d\omega\,dq. \tag{2}$$

In the above integral, the vectors q^+ and q^- parameterize the post-collisional velocities and are given by

$$q^+ = \frac{1}{2}(q+|q|\omega), \quad q^- = \frac{1}{2}(q-|q|\omega), \tag{3}$$

whereas the deflection angle θ is the angle between the unit vectors $q/|q|$ and ω.

The precise form of the kernel β, which characterizes the details of the binary interactions, depends on the physical properties of the gas. In the case of inverse k-th power forces between particles the kernel has the form

$$\beta(|q|,\theta) = b_\alpha(\theta)|q|^\alpha, \tag{4}$$

where $\alpha = (k-5)/(k-1)$. In many applications the most interesting case is the variable hard sphere(VHS) model [1] i.e. $b_\alpha(\theta) = C_\alpha$ where C_α is a positive constant. The case $\alpha = 0$ is referred to as Maxwellian gas whereas the case $\alpha = 1$ yields the Hard Sphere gas.

The second result we will use in the derivation of the method is the following [14]

Proposition 2.1 *Let* $\mathrm{Supp}(f(v)) \subset \mathcal{B}(0,R)$, *where* $\mathcal{B}(0,R)$ *is the ball of radius* R *centered in the origin, then*

$$Q(f,f)(v) = \int_{\mathcal{B}(0,2R)}\int_{S^2} B(|q|,\theta)[f(v+q^+)f(v+q^-) - f(v)f(v+q)]\,d\omega\,dq,$$

with $v+q^+, v+q^-, v+q \in \mathcal{B}(0,(2+\sqrt{2})R)$.

Thus, in order to write a spectral approximation to (1) we consider the distribution function $f(v)$ restricted on the cube $[-T,T]^3$ with $T \geq (2+\sqrt{2})R$, assuming $f(v) = 0$ on $[-T,T]^3 \setminus \mathcal{B}(0,R)$, and extend it by periodicity to a periodic function on $[-T,T]^3$. As observed in [15], it is enough to take $T \geq (3+\sqrt{2})R/2$ to prevent period intersections.

To simplify the notation let us take $T = \pi$ and hence $R = \lambda\pi$ with $\lambda = 2/(3+\sqrt{2})$. Hereafter, we use just one index to denote the tree-dimensional sums with respect to the three-dimensional vector of integers $k = (k_1,k_2,k_3)$

$$\sum_{k=-N}^{N} := \sum_{k_1,k_2,k_3=-N}^{N}.$$

The approximate function f_N is represented as the truncated Fourier series

$$f_N(v) = \sum_{k=-N}^{N} \hat{f}_k e^{ik\cdot v}, \quad \hat{f}_k = \frac{1}{(2\pi)^3} \int_{[-\pi,\pi]^3} f(v) e^{-ik\cdot v} \, dv. \tag{5}$$

The spectral Fourier method is obtained by requiring that the residual of (1) be orthogonal to all trigonometric polynomials of degree $\leq N$ [5, 11]. Hence for $k = -N, \dots, N$

$$\int_{[-\pi,\pi]^3} \left(\frac{\partial f_N}{\partial t} - Q(f_N, f_N) \right) e^{-ik\cdot v} \, dv = 0. \tag{6}$$

By substituting (5) in (6) we get a set of Ode's for the Fourier coefficients

$$\frac{\partial \hat{f}_k}{\partial t} = \sum_{\substack{l+m=k \\ l,m=-N}}^{N} \hat{f}_l \, \hat{f}_m \hat{B}(l,m), \quad k = -N, \dots, N, \tag{7}$$

where $\hat{B}(l,m) = \hat{\beta}(l,m) - \hat{\beta}(m,m)$, and the kernel modes $\hat{\beta}(l,m)$ are given by

$$\hat{\beta}(l,m) = \int_{\mathcal{B}(0,2\lambda\pi)} \int_{S^2} \beta(|q|,\theta) e^{i(q^+\cdot l + q^-\cdot m)} \, d\omega \, dq. \tag{8}$$

Now (8) are scalar quantities depending just on the particular kernel structure. It is easy to recognize that $\hat{\beta}(l,m)$ depends only on $|l+m|$, $|l-m|$, $(l-m)\cdot(l+m))$. In the VHS case the dependence on the scattering angle disappears and (8) reduces to a one-dimensional integral [15]

$$\hat{\beta}(l,m) = C_{\lambda,\alpha} \int_0^1 r^{2+\alpha} \, \mathrm{Sinc}(\lambda\pi|l+m|r) \, \mathrm{Sinc}(\lambda\pi|l-m|r) \, dr, \tag{9}$$

where $C_{\lambda,\alpha} = (4\pi)^2 (2\lambda\pi)^{3+\alpha} C_\alpha$. From (9) it is easy to obtain the bound for $\alpha > -3$

$$|\hat{\beta}(l,m)| \leq \frac{C_{\lambda,\alpha}}{(3+\alpha)}. \tag{10}$$

It is remarkable that for integer values of $\alpha > -3$ the integral in (9) can be computed explicitly [15].

It has been shown in [15] that the spectral method defined by (7)-(8) has infinite order of accuracy if the solution is smooth. Moreover the method is such that the mass is preserved in time whereas momentum and energy are approximated with spectral accuracy. However, positivity of the solution is not guaranteed by the method. The next section is devoted to demonstrate that with a suitable use of smoothing filters we may recover this property.

3 Filtering and stability of the spectral method

Let us first set up the mathematical framework of our analysis. For $N \geq 0$, we define the space of trigonometric polynomials of degree $\leq N$ in v

$$I\!P^N = span\left\{e^{ik\cdot v} \mid -N \leq k_j \leq N,\, j = 1,2,3\right\}.$$

Moreover, let $\mathcal{P}_N : L^2([-\pi,\pi]^3) \to I\!P^N$ be the orthogonal projection upon $I\!P^N$ in the inner product of $L^2([-\pi,\pi]^3)$ (see (6)):

$$< f - \mathcal{P}_N f, \phi >= 0, \qquad \forall\, \phi \in I\!P^N.$$

We denote the L^2-norm by

$$||f||_2 = (< f, f >)^{1/2}.$$

With this definition $\mathcal{P}_N f = f_N$, where f_N is the truncated Fourier series of f (5) and the spectral method defined by equation (7) can be written in equivalent form as

$$\frac{\partial f_N}{\partial t} = Q_N^\lambda(f_N, f_N), \tag{11}$$

where $Q_N^\lambda(f_N, f_N) = \mathcal{P}_N Q^\lambda(f_N, f_N)$ and we denote by $Q^\lambda(f,f)$ the Boltzmann operator with cut-off on the relative velocity on $\mathcal{B}(0, 2\lambda\pi)$.

We will also define the smoothing operator $\mathcal{S} : I\!P^N \to I\!P^N$ for the truncated Fourier series which is defined by a multiplication of each Fourier coefficient by a factor σ_k

$$\mathcal{S}\, f_N(v) = f_N^s = \sum_{k=-N}^{N} \sigma_k \hat{f}_k e^{ik\cdot v}, \tag{12}$$

where $\sigma_k = \sigma_{k_1}\sigma_{k_2}\sigma_{k_3}$ are required to be real non-negative numbers such that $\sigma_{k_j} = \sigma_{-k_j}$, $\sigma_{k_j=0} = 1$ and $\sigma_{|k_j|} < \sigma_{|k_j-1|}, j = 1,2,3$.

Let us remark that, in general, when we approximate a non negative function by a partial sum of its Fourier series, that partial sum may be negative. We have the following well-known result [5, 11]

Proposition 3.1 *Let $f \in L^2([-\pi,\pi]^3)$, $f \geq 0, \forall\, v$. If the factors σ_k are such that*

$$1 + 2\sum_{k=1}^{N} \sigma_k \cos(k\cdot v) \geq 0, \tag{13}$$

then

$$f_N^s(v) \geq 0, \quad \forall\, v.$$

The requirement in (13) can be satisfied using the factors [5, 11]

$$\sigma_{k_j} = \left(1 - \frac{|k_j|}{N}\right), \quad j = 1, 2, 3. \tag{14}$$

These smoothing factors correspond to a nonnegative kernel K_N, the so called Fejer's kernel, given by

$$K_N(v) = \frac{1}{N^3} \prod_{i=1}^{3} \left(\frac{\sin(Nv_i/2)}{\sin(v_i/2)}\right)^2 \geq 0. \tag{15}$$

Remark 3.1 *In practice, Fejer's kernel produce an heavy smearing of the function. In most applications it is desirable to have a sharper representation of the function by using different smoothing (see section 4) at the expense of retaining some oscillations or small negative values.*

In the sequel, we will restrict our discussion to the VHS model introduced previously for $\alpha > -3$. To construct a positive spectral scheme we use the following approach.

Let us rewrite the IVP for equation (1) with cut-off in the equivalent form

$$\begin{aligned} &\frac{\partial f}{\partial t} + \mu f = J^\lambda(f, f), \qquad v \in \mathbb{R}^3,\ t > 0, \\ &f(v, t = 0) = f_0(v), \end{aligned} \tag{16}$$

with $J^\lambda(f, f) = Q^\lambda(f, f) + \mu f$. It is easy to check that for the loss part of the collision operator $Q^\lambda_-(f, f) = f R^\lambda(f)$ we have the inequality

$$R^\lambda(f) \leq C_\alpha 4\pi(2\lambda\pi)^\alpha \int_{[-\pi,\pi]^3} f(v)\, dv = C_\alpha 4\pi(2\lambda\pi)^\alpha \rho.$$

Thus for $\mu \geq C_\alpha 4\pi(2\lambda\pi)^\alpha \rho$, $J^\lambda(f, f)$ is a positive monotone operator in the sense that

$$J^\lambda(f, f) \geq J^\lambda(g, g) \geq 0 \quad \text{if} \quad f \geq g \geq 0.$$

Next we have

Lemma 3.1 *Let $f, g \in L^2([-\pi, \pi]^3)$, $f \geq g \geq 0$, then $J^{\lambda,s}_N(f, g) := \mathcal{S}\, J^\lambda_N(f, g) \in \mathbb{P}_N$, $J^{\lambda,s}_N(f, f) \geq J^{\lambda,s}_N(g, g) \geq 0$ and*

$$||J^{\lambda,s}_N(f, g)||_2 \leq C||f||_2||g||_2.$$

Proof
The first statement follows immediately from Proposition 3.1 since for $f \geq g \geq 0$,

$$J_N^{\lambda,s}(f,f) = \mathcal{S}\mathcal{P}_N J^\lambda(f,f) \geq \mathcal{S}\mathcal{P}_N J^\lambda(g,g) = J_N^{\lambda,s}(g,g) \geq 0.$$

Next we get from $J_N^{\lambda,s}(f,g) = Q_N^{\lambda,s}(f,g) + \mu(f_N^s + g_N^s)/2$,

$$||J_N^{\lambda,s}(f,g)||_2 \leq ||Q_N^{\lambda,s}(f,g)||_2 + C_2||f||_2||g||_2. \tag{17}$$

In the previous inequality we have used the fact that for any function $f \in L^2([-\pi,\pi]^3)$, $f \geq 0$ we have

$$||f_N^s||_2 \leq ||f_N||_2 \leq ||f||_2, \quad \rho = ||f||_1 \leq (2\pi)^{3/2}||f||_2.$$

In addition the following estimate holds [15]

$$||Q_N^{\lambda,s}(f,g)||_2 \leq C_1||f||_2||g||_2, \tag{18}$$

that together with (17) gives the result.

■

We can now state the main results regarding the stability of the method

Theorem 3.1 *There exists a unique positive solution $f_N(t,v) \in C^1([0,T],\mathbb{P}^N)$, with $||f_N||_1 = \rho$, for arbitrary time $T > 0$ to the initial value problem*

$$\begin{aligned} \frac{\partial f_N}{\partial t} + \mu f_N &= J_N^{\lambda,s}(f_N,f_N), \qquad v \in \mathbb{R}^3,\ t>0, \\ f_N(v,t=0) &= f_{0,N}^s(v), \end{aligned} \tag{19}$$

provided that $f_0 \in L^2([-\pi,\pi]^3)$ is non negative, $||f_0||_1 = \rho$, and that the smoothing operator $\mathcal{S}$ satisfies (13).

Proof
First we show that the projected (smoothed) operator $J_N^{\lambda,s}(f_N,f_N)$ will preserve the mass in time. In fact, we have

$$\int_{[-\pi,\pi]^3} Q_N^{\lambda,s}(f_N,f_N)\,dv = \sum_{k=-N}^{N} \sigma_k \sum_{\substack{l+m=k \\ l,m=-N}}^{N} \hat{f}_l \hat{f}_m \hat{B}(l,m) \int_{[-\pi,\pi]^3} e^{ikv}\,dv \tag{20}$$

$$= (2\pi)^3 \sum_{m=-N}^{N} \hat{f}_{-m}\hat{f}_m \hat{B}(-m,m) = 0, \tag{21}$$

since $\hat{B}(-m, m) = 0$, $\forall m$. The last identity is an easy consequence of the fact that $\hat{\beta}(m, m)$ depends only on $|m|$. Thus

$$\int_{[-\pi,\pi]^3} J_N^{\lambda,s}(f_N, f_N)\, dv = \mu \int_{[-\pi,\pi]^3} f_N^s\, dv = \mu \int_{[-\pi,\pi]^3} f_N\, dv = \mu\rho.$$

Next we observe that from Lemma 3.1 and mass conservation the existence of a unique positive solution $f_N(t, v) \in C^1([0, T], L^2([-\pi, \pi]^3)$ follows by standard arguments [7]. In particular this solution can be represented as a Wild sum [9]

$$f_N(v, t) = e^{-\mu t} \sum_{n=0}^{\infty} (1 - e^{-\mu t})^n f_N^{(n)}(v), \tag{22}$$

where

$$f_N^{(n+1)} = \frac{1}{n+1} \sum_{j=0}^{n} \frac{1}{\mu} J_N^{\lambda,s}(f_N^{(j)}, f_N^{(n-j)}), \quad f_N^{(0)} = f_N(v, t = 0). \tag{23}$$

Finally, since all the terms in the sums (23) are in $I\!\!P_N$ we can conclude that $f_N(v, \cdot) \in I\!\!P_N$ for $t > 0$.

■

4 Smoothing techniques

First, we observe that the scheme we have introduced in the previous section represents a generalization of the Fourier-Galerkin method presented in [15]. As we have emphasized, the original spectral method is spectrally accurate but does not preserve the positivity of the solution exactly. However, for smooth solutions, positivity is preserved with spectral accuracy (a measure of the lack of positivity is obtained by comparing the integral of the function with its L^1 norm. The first one is conserved by the method, while the second differs from the first for functions which are not always positive). On the contrary, if the smoothing filter satisfies (13), the new smoothed scheme preserves the positivity of the initial data. Clearly a serious loss of accuracy is expected for the smoothed positive scheme. However, we will show in our experiments that this lack of accuracy is mainly originated by the smoothed projection of the initial data and not by the smoothed time evolution which gives acceptable approximations.

4.1 Implementation of the scheme

The Fourier representation of the solution allows to reconstruct the function on a finer mesh than the one used for computation, almost with no additional cost. One may view the reconstruction either as a continuous representation of the solution from its Fourier coefficients, or as a trigonometric interpolation at the computational nodes.

The values of the function at the nodes are obtained from the Fourier modes through the discrete Fourier transform (which can be efficiently computed by FFT)

$$f_N(v_m) = \sum_{k=-N}^{N-1} \hat{f}_k e^{(i\pi k\cdot m/N)}, \tag{24}$$

where $v_m = \pi m/N$, $m = (m_1, \cdots, m_d)$, $k = (k_1, \cdots, k_d)$, $(2N)^d$ is the total number of modes, and d is the dimension in velocity space. As usual, we have used the form (24), which has $(2N)^d$ degrees of freedom, instead of (5), which has $(2N+1)^d$ degrees of freedom, because it corresponds directly to the way spectral methods are implemented.

The evolution equation for the Fourier modes for the initial value problem are the following

$$\frac{d\hat{f}_k}{dt} = \hat{Q}_k, \tag{25}$$

$$\hat{f}_k(0) = \hat{f}_k^0, \tag{26}$$

where $\hat{f}_k^0$ are the Fourier coefficients of the initial condition, and $\hat{Q}_k$ is the right hand side of (7). The new smoothed version of the evolution equation is given by Eq. (19), which in Fourier space has the following representation

$$\frac{d\hat{f}_k}{dt} = \sigma_k \hat{Q}_k - \mu(1-\sigma_k)\hat{f}_k, \tag{27}$$

$$\hat{f}_k(0) = \sigma_k \hat{f}_k^0. \tag{28}$$

Theorem 3.1 ensures that by evolving the Fourier coefficients according to (27)-(28), the corresponding function is positive, provided the initial function is positive, and the coefficients σ_k correspond to a positive kernel, such as Fejer's kernel (15).

4.2 Numerical results

We consider here two test problems for the space-homogeneous Boltzmann equation (2D in velocity). The first consists of Maxwell molecules with the following initial condition

$$f(v,0) = \frac{v^2}{\pi\sigma^4}\exp(-v^2/\sigma^2).$$

In this case an exact solution is known [13], and is given by

$$f(v,t) = \frac{1}{2\pi S^2\sigma^2}\left(2S - 1 + \frac{1-S}{2S}\frac{v^2}{\sigma^2}\right)\exp\left(-\frac{v^2}{2S\sigma^2}\right),$$

with $S(t) = 1 - \exp(-\sigma^2 t/8)/2$. We used $\sigma = 2\pi/11$.

If we perform the computation with the Fourier-spectral method, using 16^2 modes, we obtain a good approximation of the exact solution at the nodes. The positivity error is measured by the quantity

$$\epsilon_p := \frac{\sum |f_N(v_m)| - \sum f_N(v_m)}{\sum f_N(v_m)},$$

and its evolution is shown in Fig. 1. As it is expected, the positivity error is quite small, even for a grid as coarse as 16^2.

Positivity error can be eliminated by solving system (27)-(28), instead of (25)-(26). In fact according to Theorem 3.1, the solution stays positive at any time in this case.

The result of the computation performed according to (27)-(28) is shown in Fig. 2, in the case of a 32^2 mesh. The positivity error is zero, but the accuracy of the scheme is extremely poor.

As we mentioned before, the spectral method provides a continuous representation of the solution. Once the Fourier coefficients of the numerical solution are obtained, the function may be computed as

$$f_N(v,t) = \sum_{k=-N}^{N-1} \hat{f}_k(t) e^{ik\cdot v}.$$

Such reconstruction, however, may introduce spurious oscillations in the solution. To show this effect we plot a magnified picture of the numerical solution in Fig. 3. Note that the numerical solution is quite accurate on the nodes, even with 16^2 modes. The oscillations (and positivity error) become extremely small when the mesh is refined. In particular the oscillations are strongly damped by the time evolution of the method.

We remark that the main cause of oscillations (and negativity of the solution) lies in the oscillatory behavior of the initial condition. Similarly, the main cause of loss of accuracy for the smoothed solution lies in the loss of accuracy in the smoothed initial data.

Two emphasize this effect we consider a second test problem. We solve the Boltzmann equation for hard sphere molecules (2D in velocity). The initial condition is the sum of two Maxwellian,

$$f(v,0) = \frac{1}{2(2\pi\sigma^2)} \left[\exp\left(-\frac{|v - 2\sigma e_1|^2}{2\sigma^2} \right) + \exp\left(-\frac{|v + 2\sigma e_1|^2}{2\sigma^2} \right) \right],$$

with $\sigma = \lambda\pi/6$ and e_1 is the unit vector in the x direction. We use 32^2 Fourier modes. First, we compare the solution of Eqs. (25)-(26) to the solution obtained by solving Eq. (25) with the smoothed initial condition (28). We test different kinds of smoothing, namely Fejer's smoothing, given by Eq. (14), Lanczos smoothing, given by

$$\sigma_k = \frac{\sin k\pi/N}{k\pi/N}, \quad k = -N, \dots, N-1, \tag{29}$$

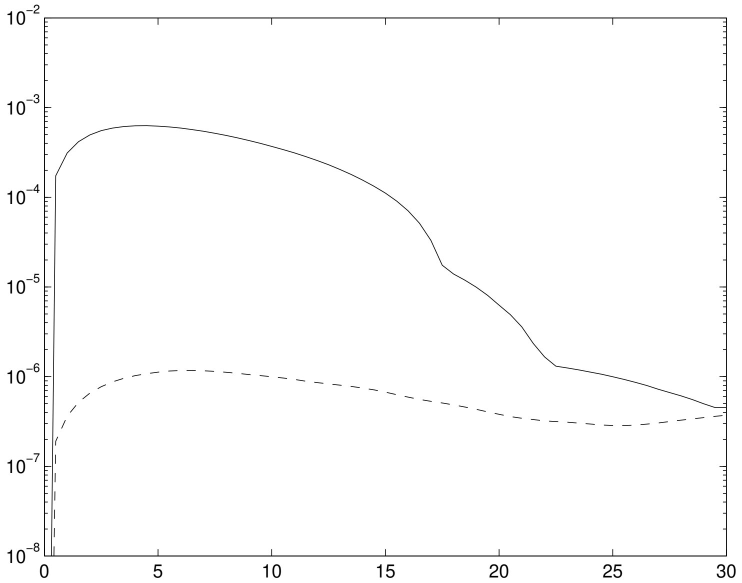

Figure 1: Positivity error vs time for the unsmoothed method with a 16^2 mesh (continuous line) and a 32^2 mesh (dashed line).

and raised cosine smoothing, given by

$$\sigma_k = \frac{1 + \cos k\pi/N}{2}, \quad k = -N, \dots, N-1. \tag{30}$$

The result of the computation is shown in Fig. (4). Raised cosine gives very smooth results, with virtually no oscillations nor positivity error. Note, however, that the smoothing of the initial condition produced a dramatic degradation of accuracy (see Fig. 5).

Finally we present in Fig. (6) the same computations by comparing the solution of Eqs. (25)-(26) to the solution obtained by solving the smoothed method (27) with the initial condition (26). Although the initial data is not smoothed we can observe that at $t = 1$ the oscillations have almost disappeared and we have essentially no oscillations or positivity error for all the filters we have used. In particular, we emphasize that this approach permits to reduce strongly the degradation of accuracy introduced by the smoothing filters (see Fig. 7).

5 Conclusions

We have introduced a new smoothed spectral scheme for the numerical solution of the homogeneous Boltzmann equation. This scheme represents a generalization of the original Fourier-Galerkin scheme introduced in [14, 15] with better stability properties. For the new scheme we have proved that the solution, if initially positive and if the smoothing is

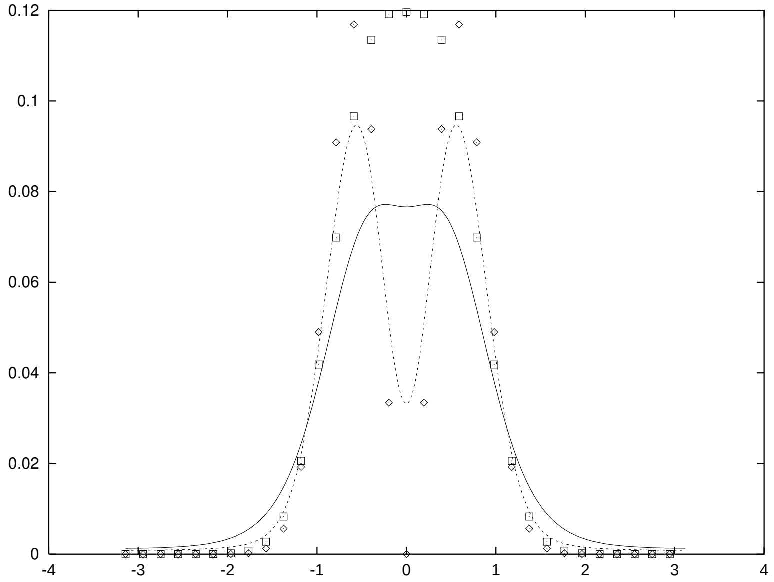

Figure 2: Positivity but loss of accuracy using Fejer smoothing. Density function f, at time $t = 0, 6$ with $N = 32$ modes per direction. Markers: initial condition (diamonds) and exact solution (squares). Lines: initial condition (dotted line) and numerical solution (continuous line).

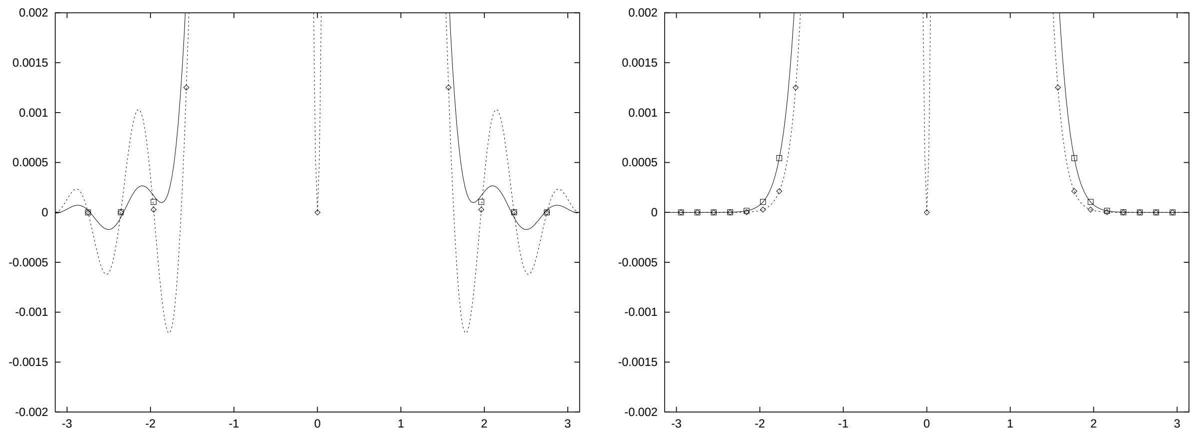

Figure 3: Decay of oscillations for the unsmoothed method. Initial data (dots) and numerical result (line) at time $t = 6$. The markers represent the exact solution on the grid. N=16 modes per direction (left), N=32 modes per direction (right).

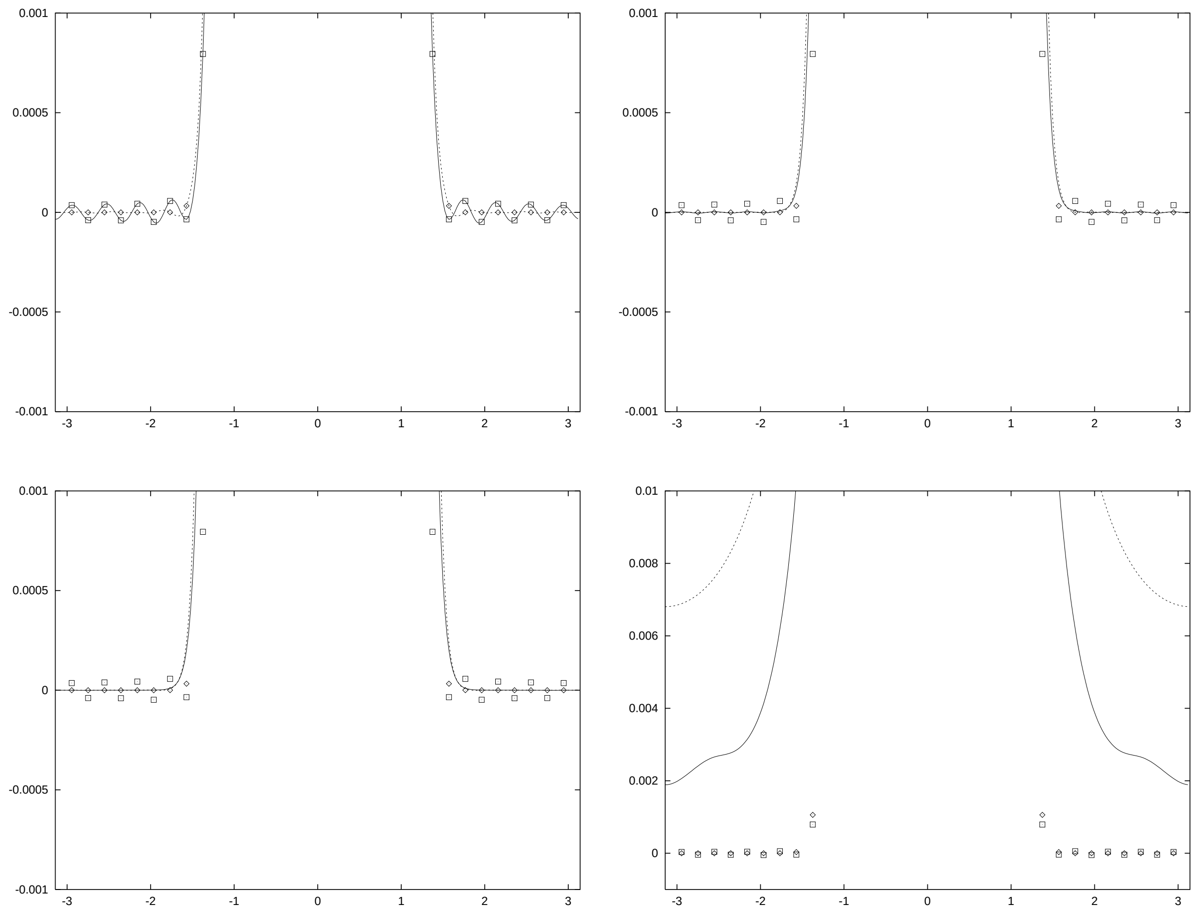

Figure 4: Effect of the smoothing of the initial condition. Initial condition: sum of two Maxwellian. Hard Sphere molecules. The markers denote initial condition (diamonds) and unsmoothed solution at time $t = 1$ (squares) on the grid points. Unsmoothed (top left), Lanczos smoothing (top right), raised cosine smoothing (bottom left), Fejer smoothing (bottom right).

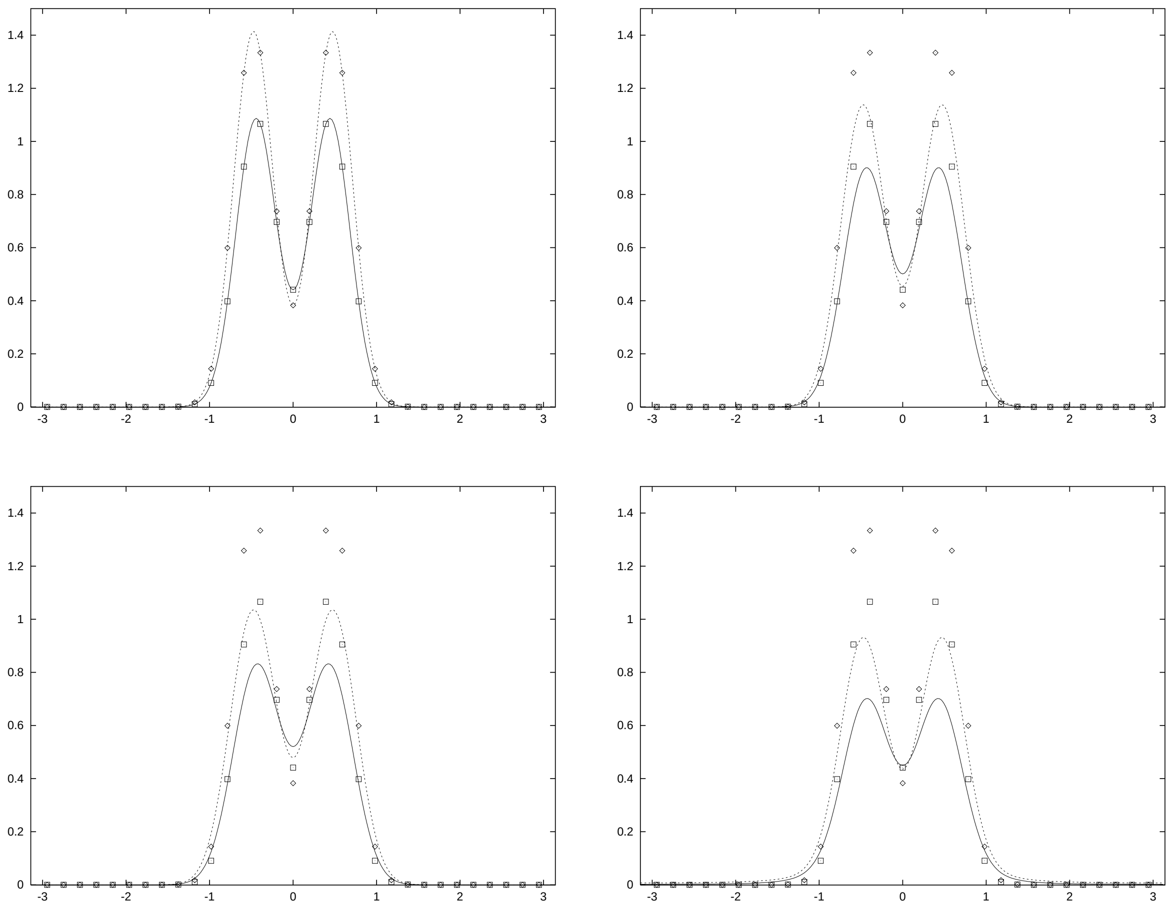

Figure 5: Same as previous figure, on a smaller scale.

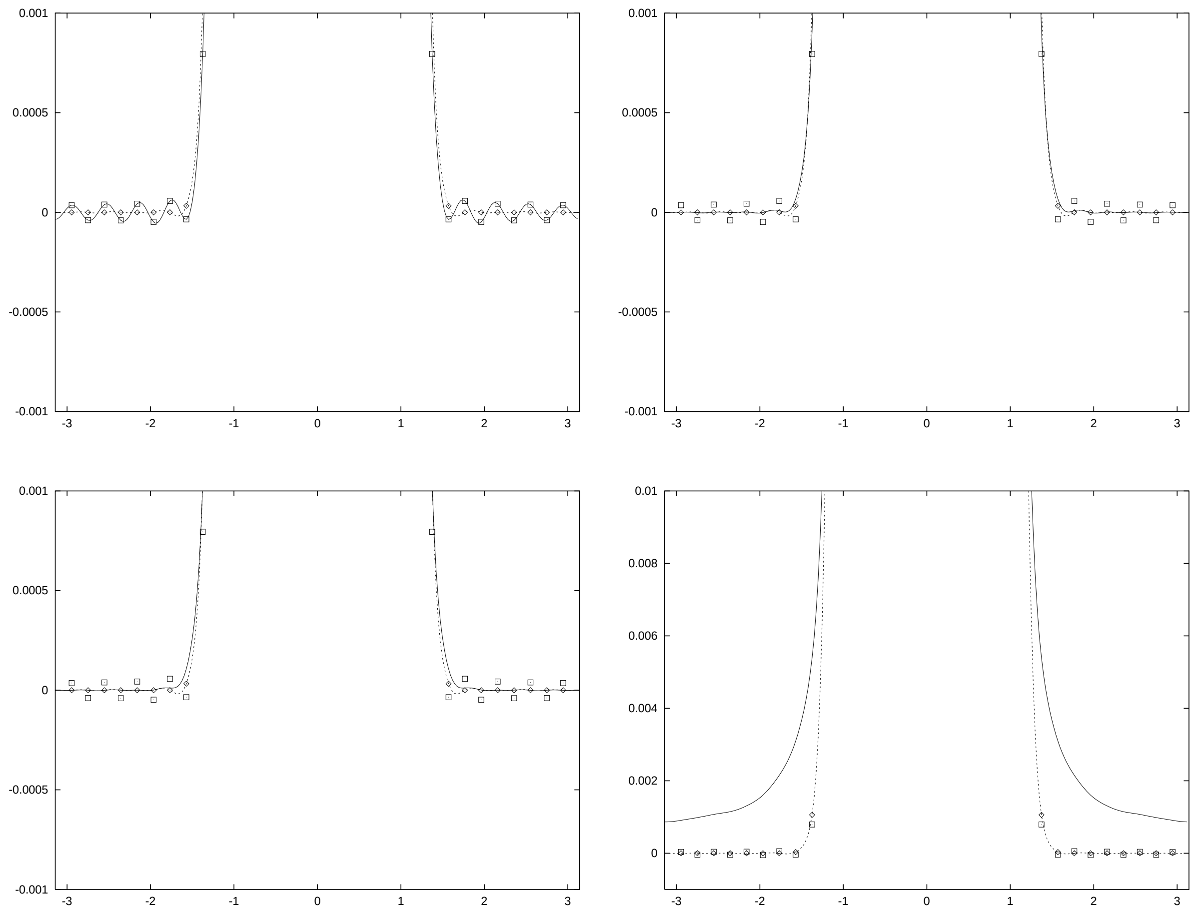

Figure 6: Effect of the smoothing of the method. Initial condition: sum of two Maxwellian. Hard Sphere molecules. The markers denote initial condition (diamonds) and un-smoothed solution at time $t = 1$ (squares) on the grid points. Un-smoothed (top left), Lanczos smoothing (top right), raised cosine smoothing (bottom left), Fejer smoothing (bottom right).

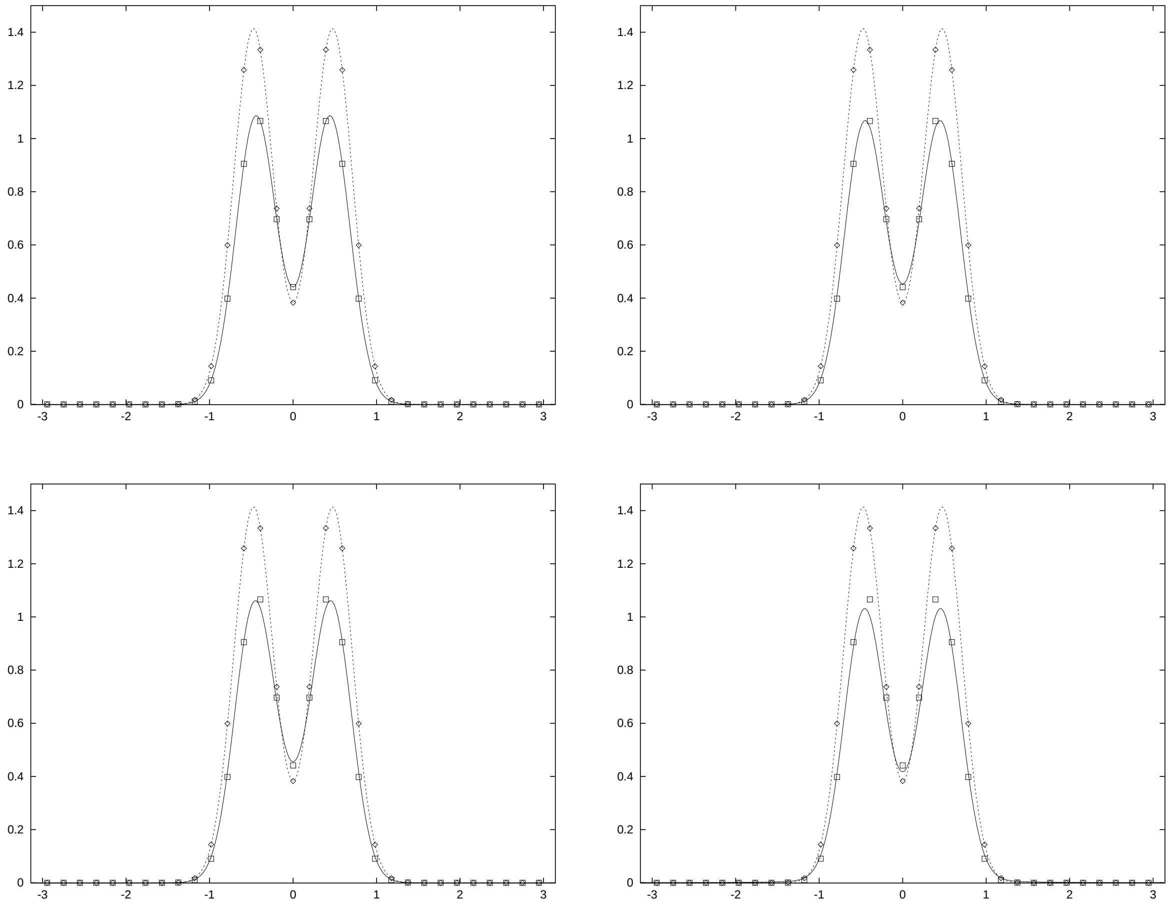

Figure 7: Same as previous figure, on a smaller scale.

strong enough, remains positive in time. Clearly, the use of smoothing filters has to be done carefully since they produce a heavy smearing of the solution that may destroy the spectral accuracy of the scheme. When the solution is smooth there is no need in general to use any smoothing in the method but in presence of discontinuities in the velocity space [18] the use of a week form of smoothing may give a better representation of the solution. Numerical results suggest the use of filtering tecniques on the spectral scheme but not on the initial data. This issue will be addressed in a future paper [16].

Acknowledgments
L. Pareschi would like to thank C. Villani for helpful discussions.

References

[1] G.A. BIRD *Molecular gas dynamics*, Clarendon Press, Oxford, (1994).

[2] A.V. BOBYLEV *The method of the Fourier transform in the theory of the Boltzmann equation for Maxwell molecules*, Dokl. Akad. Nauk SSSR, 225, 6, (1975), pp. 1041–1044.

[3] A.V. BOBYLEV, RJASANOV *Difference scheme for the Boltzmann equation based on the Fast Fourier Transform*, Eur. J. Mech., B/Fluids, 16, 2, (1997), pp. 293–306.

[4] C. BUET *A discrete velocity scheme for the Boltzmann operator of rarefied gas dynamics*, Trans. Theo. Stat. Phys., 25, 1, (1996), pp. 33–60.

[5] C. CANUTO, M.Y. HUSSAINI, A. QUARTERONI, T.A. ZANG Spectral methods in fluid dynamics, Springer Verlag, New York (1988).

[6] C. CERCIGNANI The Boltzmann equation and its applications, Springer-Verlag, Berlin, (1988).

[7] C. CERCIGNANI, R.ILLENR, M.PULVIRENTI, The mathematical theory of dilute gases, Springer-Verlag, New York, (1995).

[8] E. GABETTA, L. PARESCHI *The Maxwell gas and its Fourier transform towards a numerical approximation*, Waves and stability in continuous media, Bologna 1993, Ser. Adv. Math. Appl. Sci., 23, (1994), pp. 197–201.

[9] E. GABETTA, L. PARESCHI, G. TOSCANI *Relaxation schemes for nonlinear kinetic equations*, SIAM J. Numer. Anal., 34, 6, (1997), pp. 1967–2011.

[10] D.GOLDSTEIN, B.STURTEVANT, J.E.BROADWELL *Investigation of the motion of discrete velocity gases*, Rarefied Gas Dynamics: Theoretical and Computational Techniques, edited by E.P.Munz, D.P.Weaver, H.D.Campbell, 118, AIAA, Washington DC, (1989), p.100.

[11] D. GOTTLIEB, S. A. ORSZAG Numerical Analysis of Spectral Methods: Theory and Applications, SIAM CBMS-NSF Series (1977).

[12] Y.N. GRIGORIEV, A.N. MIKHALITSYN *A spectral method of solving Boltzmann's kinetic equation numerically*, U.S.S.R. Comput. Maths. Math. Phys., 23, 6, (1983), pp. 105–111.

[13] M. H. ERNST *Exact solutions of the nonlinear Boltzmann equation and related kinetic models*, Nonequilibrium Phenomena I. The Boltzmann equation, North-Holland, (1983), pp. 52–119.

[14] L.PARESCHI, B.PERTHAME *A Fourier spectral method for homogeneous Boltzmann equations*, Trans. Theo. and Stat. Phys., 25, 5, (1996), pp. 369–383.

[15] L.PARESCHI, G.RUSSO *Numerical solution of the Boltzmann equation I: Spectrally accurate approximation of the collision operator*, SIAM J. Num. Anal. to appear.

[16] L.PARESCHI, G.RUSSO *Numerical solution of the Boltzmann equation II: Uniformly accurate second order schemes*, work in preparation.

[17] F.ROGIER, J.SCHNEIDER *A direct method for solving the Boltzmann equation*, Trans. Theo. Stat. Phys., 23, 1-3, (1994), pp. 313–338.

[18] S. TAKATA, Y.SONE, K.AOKI *Numerical analysis of a uniform flow of a rarefied gas past a sphere on the basis of the Boltzmann equation for hard-sphere molecules*, Phys. Fluids A, 5, 3, (1993), pp. 716-737.